Advance Sustainable Science, Engineering and Technology (ASSET)
Vol. 8, No.1, January 2026, pp. 0260108-01 ~ 0260108-015
ISSN: 2715-4211 DOI: https://doi.org/10.26877/asset.v8i1.2163

Comparative Performance Evaluation of Electric Powertrains in ICE Motorcycle Conversion

Muhammad Rizani Rusli[1*], Eko Henfri Binugroho[2], Mochamad Ari Bagus Nugroho[1], Himmawan Sabda Maulana[2], Raden Sanggar Dewanto[2], Teguh Hady Ariwibowo[2], Dadet Pramadihanto[3], Mentari Putri Jati[5]

[1]Department of Electrical Engineering Politeknik Elektronika Negeri Surabaya, Surabaya 60111, Indonesia

[2]Department of Mechanical and Energy Engineering Politeknik Elektronika Negeri Surabaya, Surabaya 60111, Indonesia

[3]Department of Informatics and Computer Engineering, Politeknik Elektronika Negeri Surabaya, Surabaya 60111, Indonesia

[5]Department of Electro-Optical Engineering, National Taipei University of Technology, Taipei City, Taiwan

*rizani@pens.ac.id

Abstract. Electrifying Indonesia's motorcycle fleet is critical for reducing urban emissions and fossil fuel dependence. This study experimentally evaluates three powertrain configurations—hub motor, continuously variable transmission (CVT), and single-gear ratio—for converting internal combustion engine (ICE) motorcycles to electric two-wheelers (E2W). Using a Honda Vario 125 platform with a 72 V, 3 kW Brushless DC motor and 1.44 kWh lithium-ion battery, performance was assessed via chassis dynamometer and real-world urban road tests. The single-gear ratio configuration demonstrated superior overall performance, achieving 5.15 kW peak wheel power, 188.7 N·m torque, fastest acceleration (0–128 km/h in 22 s), and highest energy efficiency (37.0 km/kWh), enabling a 51.8 km range per charge. The hub motor excelled in top speed, while the CVT consistently underperformed. Benchmarking shows up to 104 % efficiency improvement over prior designs. These results provide quantitative guidance for converters, manufacturers, and policymakers, establishing the single-gear ratio as the optimal solution for urban and commercial E2W applications and supporting sustainable mobility initiatives.

Keywords: ICE motorcycle conversion, electric powertrain, BLDC motor, dynamometer testing, experimental performance analysis

(Received 2025-06-15, Revised 2025-11-13, Accepted 2025-11-26, Available Online by 2026-01-06)

1. Introduction

The global transition toward sustainable transportation is a critical imperative for mitigating climate change. The transport sector, the world's largest consumer of fossil fuels, accounts for more than 91% of global oil-based energy consumption, making it a primary contributor to carbon emissions [1]. This challenge is particularly acute in Indonesia, where transportation is the second-largest source of emissions, contributing approximately 28.4% of the nation's total carbon output [2–4]. In response, the adoption of electric vehicles (EV)—notably battery electric vehicles (BEV)—has been promoted as a pivotal strategy to decarbonize transport, reduce dependence on fossil fuels, and improve urban air quality [1,2,5,6].

The Indonesian government has enacted proactive policies to accelerate this transition [7]. Central to these efforts is Presidential Regulation (Perpres) No. 79/2023, which amends Perpres No. 55/2019 on accelerating the battery-based electric motor vehicle program. This regulation advances EV adoption through fiscal incentives, subsidies, and charging infrastructure development, while simultaneously promoting domestic industrialization [8]. Complementary regulations, such as the Minister of Energy and Mineral Resources Regulation No. 1/2023 and the Minister of Industry Regulation No. 21/2023, further govern charging infrastructure and provide purchase incentives [9,10]. Collectively, these policies aim to establish a supportive ecosystem aligned with Indonesia's sustainable development goals [11–13].

Within this policy landscape, two-wheeled vehicles represent a sector of singular importance. Motorcycles constitute the backbone of transportation in Indonesia, particularly in dense urban environments with congested road networks. The country hosts the world's third-largest motorcycle fleet, with registrations surpassing 132.4 million units in 2023 and an annual growth of over 5 million units [2,14–17]. The market is dominated by automatic scooters, valued for their affordability and ease of use [18,19]. However, the overwhelming majority employ internal combustion engines (ICEs), exacerbating fossil fuel dependence and urban air pollution. Electrifying this fleet is therefore not merely an option but a necessity for meeting national emission targets.

One promising and scalable pathway is the conversion of existing ICE two-wheelers (ICE-TW) into electric two-wheelers (E2W). This approach reduces the high upfront costs associated with new EV purchases, thereby improving accessibility, while simultaneously delivering immediate environmental benefits through reduced tailpipe emissions [20,21]. Conversion also extends the service life of existing vehicle frames, mitigating waste and lowering the environmental footprint of new manufacturing [22]. From an economic perspective, it provides a cost-effective route for individuals and commercial operators, such as logistics and delivery fleets, to transition toward electric mobility [23].

A key technical challenge in such conversions lies in the selection and integration of an appropriate electric powertrain. The Brushless DC (BLDC) motor is widely favored for its high efficiency, torque density, and durability, making it suitable for the demanding duty cycles of urban mobility [20,22,24–26]. However, system performance depends not only on the motor itself but also on the associated transmission configuration. Options range from direct-drive hub motors, which provide simplicity and efficiency but limited speed range, to geared systems that enable speed–torque trade-offs at the expense of greater complexity, and Continuously Variable Transmissions (CVTs), which allow smooth acceleration but may incur efficiency losses [27–31]. A comparative assessment of these configurations under standardized conditions remains a significant gap in the literature, particularly with respect to the ubiquitous automatic scooter platform.

While prior studies have demonstrated the technical feasibility of ICE-TW conversions and documented the performance of individual motor types [21–23,32], rigorous comparative evaluations of complete powertrain configurations remain scarce. In particular, empirical studies capturing real-world trade-offs between traction motors and transmission systems under standardized testing conditions are limited.

This study seeks to address this gap by providing systematic experimental evidence from a standardized conversion process. The Honda Vario 125 was selected as the base platform owing to its market dominance in Indonesia, ensuring both practical relevance and broad applicability of the findings

[33–35]. The main contributions of this paper are threefold:

1. A comprehensive empirical evaluation of key powertrain configurations for E2W conversions, assessing their impact on critical performance indicators including power, speed, wheel torque, and energy consumption.
2. Rigorous experimental data obtained from chassis dynamometer testing and real-world road trials, offering insights into efficiency and performance under both controlled and practical conditions.
3. Practical recommendations for converters, policymakers, and manufacturers on optimal powertrain configurations, thereby providing evidence-based support for national policies aimed at fostering a sustainable transportation ecosystem.

2. Methods

This section outlines the research methodology used to evaluate the performance of powertrain configurations in converting ICE-TW to E2W.

2.1. Conversion Process of ICE Two-Wheelers

This study employed a systematic experimental approach to evaluate the performance of three powertrain configurations for electric two-wheeler (E2W) conversion. The base vehicle was a 2012 Honda Vario 125, which was converted into three identical units differing only in motor and transmission type. All evaluations were conducted experimentally without the use of simulations.

Disclaimer: The reference to the commercial brand (Honda Vario) is solely for the purpose of accurately specifying the experimental platform and does not imply endorsement by the authors or their affiliated institutions.

The conversion process followed five major stages, as illustrated in Figure 1.

a. Preparation and Planning
   At this stage, the vehicle to be converted was identified, and the appropriate electric powertrain system was selected, namely hub motor (in-wheel), single-gear ratio, or continuously variable transmission (CVT). Power requirements for the Brushless DC (BLDC) motor and battery capacity were defined to align with the targeted performance specifications of the converted E2W.
b. Disassembly
   All ICE components, including the engine block, exhaust system, fuel system, and fuel tank, were completely dismantled. This step aimed to prepare the motorcycle frame, free sufficient space for new components, and ensure safety in subsequent installation.
c. System Design
   Design and planning focused on the calculation and placement of key E2W components such as the lithium-ion battery pack, motor controller unit (MCU), and DC–DC converter. Placement was optimized to preserve vehicle balance, ensure mechanical integrity, and facilitate maintenance. A custom swing arm was designed to accommodate the electric powertrain, taking into account structural strength, installation dimensions, weight optimization, and modularity. The design was modeled using CAD software, and manufacturing employed aluminium alloy or mild steel through cutting, forming, welding, and surface finishing processes such as anodizing or painting.
d. Manufacturing and Installation
   The fabricated swing arm was implemented, followed by the installation of the BLDC motor and chosen transmission system. The battery pack was strategically mounted—typically under the seat—to optimize weight distribution and safety. The MCU, sensors, and wiring harness were installed to integrate the motor, battery, and controller into a single system.
e. Testing and Validation
   The electrical and mechanical systems underwent rigorous functional testing, including motor and controller verification, swing arm load performance, and throttle calibration. Standard safety systems and the 12 V auxiliary system (headlights, indicators, horn, and speedometer) were also validated. Finally, overall system performance was tested using both chassis dynamometer and road trials. The dynamometer testing technique followed a steady-state power sweep method. These

evaluations measured wheel torque, acceleration, energy consumption, and driving range under controlled and real-world conditions.

Through this staged methodology, the ICE two-wheeler was systematically converted into an electric two-wheeler, enabling a fair and reproducible comparison of the three powertrain configurations.

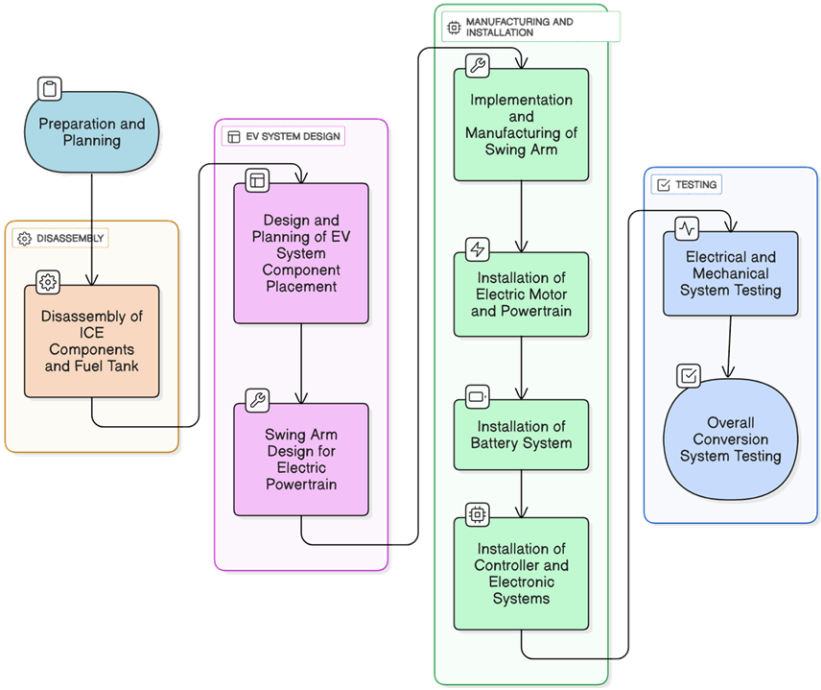

Figure 1. Conversion Process Diagram

2.2. System Design of EV Conversion from ICE Two-Wheeler

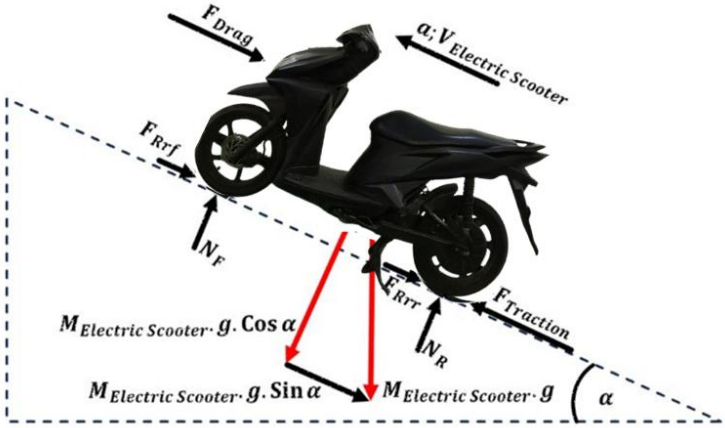

Figure 2. Dynamic Longitudinal Free Body Diagram

The system design for converting an ICE-TW into an E2W integrates several key components to ensure optimal performance and operational reliability. A longitudinal dynamic free-body diagram, as seen in Figure 2, was employed to quantify the forces acting on the vehicle during motion, including aerodynamic drag, rolling resistance, gradient resistance, and inertia. This analysis provides the basis for motor and battery selection.

$$F_{traction} = F_{drag} + F_{RollingResistance} + F_{Grade} + F_{inertia} \quad (1)$$

Where

$$F_{drag} = \frac{1}{2} . \rho . C_d . A_f . V_{ElectricScooter}{}^2 \quad (2)$$

$$F_{RollingResistance} = C_{RR} . M_{ElectricScooter} . g . \cos\alpha \quad (3)$$

$$F_{Grade} = M_{ElectricScooter} . g . \sin\alpha \quad (4)$$

$$F_{Inertia} = M_{Inertia} . a \quad (5)$$

$$M_{Inertia} = 1.15 . M_{ElectricScooter} \quad (6)$$

The traction force ($F_{traction}$) can be calculated using equations (1)-(6), where F_{drag} is the aerodynamic drag force, $F_{RollingResistance}$ is the rolling resistance force, F_{Grade} is the gravitational force on inclined roads, and $F_{inertia}$ is inertia due to the vehicle's acceleration. While, ρ is air density, C_d is the drag coefficient, A_f is the frontal area, $V_{ElectricScooter}$ is E2W's speed, C_{RR} is the rolling resistance coefficient, $M_{ElectricScooter}$ is the mass of E2W, α is road grade, and a is acceleration.

$$\tau_{wheel} = F_{traction} . r \quad (7)$$

$$\tau_{motor} = 1.2 . GearRatio . \tau_{wheel} \quad (8)$$

$$\omega_{wheel} = \frac{V_{ElectricScooter}}{r} \quad (9)$$

$$\omega_{motor} = \frac{1}{GearRatio} . \omega_{wheel} \quad (10)$$

$$P_{motor} = \tau_{motor} . \omega_{motor} . 1.2 \quad (11)$$

The corresponding wheel torque and power demand are calculated using equations (7)-(11), where τ_{wheel} is the torque wheel, τ_{motor} is the motor torque, r is wheel radius, ω_{wheel} is the wheel speed, ω_{motor} is the motor speed, and P_{motor} is the motor power.

Table 1. The Detailed Specifications of the selected components for ICE-TW to E2W conversion

Component	Specification	Key Features / Rationale
Motor	3000 W BLDC	High efficiency, high torque density; suitable for urban cycles
Battery Pack	Lithium-ion, 72 V, 20 Ah (1.44 kWh)	Range ≈ 50 km/charge; high energy density, lightweight
BMS	Integrated with battery	Cell balancing, overcharge/discharge protection, thermal monitoring
MCU	Votol EM150	Six-step drives, 150 A continuous, 380 A peak; sinusoidal control with flux-weakening
DC–DC Converter	72 V → 12 V	Powers auxiliary loads; high efficiency, low ripple
Charger	Off-board, 84 V, 5 A (220 V AC input)	Reduces onboard weight; safe and efficient

Based on these calculations, a 3000 W BLDC motor was selected for the conversion due to its high efficiency, compact size, and torque density [20,22,24–26,36]. Battery capacity was determined from estimated energy consumption. A lithium-ion battery rated at 72 V, 20 Ah (1.44 kWh) was selected, providing ~50 km range per charge at ~25 km/kWh. Lithium-ion technology offers high energy density, long cycle life, fast charging, and thermal stability [37]. An integrated Battery Management System (BMS) regulates charge/discharge cycles, balances cells, and protects against overcharge, over-discharge, and thermal stress [38]. The Motor Controller Unit (MCU) manages power delivery between the battery and motor, ensuring accurate speed and torque control. The Votol EM150 MCU was

employed, capable of 150 A continuous current and 380 A peak phase current. The controller applies sinusoidal control with flux-weakening to extend operational speed range [39]. A DC–DC converter steps down the high-voltage battery supply to 12 V for auxiliary loads such as headlights, turn signals, dashboard, and horn. High efficiency and low voltage ripple are required to ensure stable auxiliary operation [37,40,41]. For the charging system, an off-board charger rated at 84 V and 5 A was connected to a 220 V AC single-phase source. The off-board configuration avoids onboard weight and volume penalties while ensuring user convenience and safety [42]. The complete system specifications are listed in Table I.

2.3. Powertrain Configurations

The powertrain configuration is a decisive factor in determining the performance and efficiency of an electric two-wheeler (E2W). This study employed two types of BLDC motors—outer rotor and inner rotor—integrated into three transmission configurations: hub/in-wheel, continuously variable transmission (CVT), and single-gear ratio systems

2.3.1. Motor Traction Specification

The outer rotor BLDC motor, as seen in Figure 3 (a), commonly applied in hub motor systems, features an internal stator and external rotor magnets. This design delivers high torque density, smooth rotation with low cogging torque, and high efficiency. It also requires lower nominal current at rated speed, reducing power losses and thermal stress during operation. Nevertheless, the integrated rotor–magnet structure presents challenges for cooling and mechanical stability, requiring careful design considerations [43–45].

The inner rotor BLDC motor, as seen in Figure 3 (b), used in CVT and gear-ratio systems, positions the rotor magnets internally with stator windings on the outside. This configuration enhances heat dissipation and reduces rotor inertia, enabling faster dynamic response and sustained performance under variable driving conditions. While it offers compactness and high torque output, its limitations include higher cogging torque and the need for stronger permanent magnets to achieve sufficient flux density [43].

(a) (b)

Figure 3. Motor tractions : (a) BLDC outer rotor (b) BLDC inner rotor

Both motors in this study as seen in Figure 3 were rated at 72 V and 3 kW nominal power, with efficiencies above 90%, ensuring comparability across configurations. The outer rotor unit delivered a higher maximum torque (≈185 N·m) suitable for direct wheel integration, while the inner rotor unit provided moderate torque (≈50 N·m) but higher rotational speed (up to 6000 rpm), making it more suitable for geared or CVT applications.

2.3.2. Transmission Configuration

Three transmission configurations were tested, each integrated with a custom swing arm to ensure compatibility with the base motorcycle platform:

a. Hub/In-Wheel Motor System

The hub motor integrates directly into the wheel rim, eliminating drivetrain components such as

the CVT, differential, and drive shaft. This configuration reduces mechanical losses, system weight, and complexity, thereby improving efficiency [46,47]. A custom swing arm was fabricated to ensure stability and durability as seen in Figure 4 (a).

b. Continuously Variable Transmission (CVT)
The CVT enables seamless ratio adjustments, allowing the motor to operate near its optimal efficiency point under different loads and speeds [48]. In this study, the stock CVT of the Honda Vario 125 was retained and mounted on a redesigned swing arm for integration with the electric motor as seen in Figure 4 (b). While the CVT provides flexibility, it introduces additional transmission losses and mechanical complexity

c. Single-Gear Ratio System
Leveraging the flat torque characteristics of BLDC motors, the single-gear ratio system offers a lightweight and efficient drivetrain solution [46,47]. A 13T front sprocket and 60T rear sprocket were used in this study, optimized for urban driving cycles. This configuration minimizes component mass and energy losses while lowering production costs, though it sacrifices adaptability to varying load conditions as seen in Figure 4 (c).

Overall, these three powertrain configurations represent distinct design trade-offs between simplicity, adaptability, and efficiency. Their integration with the swing arm is a critical step in ensuring the structural integrity and performance of the converted vehicle.

(a) (b) (c)

Figure 4. Motor traction, transmission, and swing arm configuration design
(a) hub / in-wheel (b) CVT (c) gear ratio

2.4. Experimental Data Evaluation

The experimental evaluation of the converted electric two-wheeler (E2W) was conducted using two complementary approaches: controlled chassis dynamometer testing and real-world road testing. These methods provided both peak performance benchmarks and practical operational insights, ensuring a comprehensive assessment of each powertrain configuration.

2.4.1. Chassis Dynamometer Test

The chassis dynamometer test was performed to determine the peak torque, power, and maximum speed of each powertrain configuration. Testing employed a Super Dyno 50LA inertia-type dynamometer with the specifications in [49], the vehicle securely mounted and the rear wheel in contact with the rotating drum.

The evaluation followed a steady-state power sweep protocol: starting from low wheel speed, throttle input was gradually increased to wide-open throttle (WOT) and maintained as the drum accelerated. This procedure enabled continuous measurement of torque and power across the full wheel-speed range. Multiple runs were conducted per configuration to ensure repeatability and statistical reliability.

All tests were carried out indoors under controlled conditions to eliminate the influence of external environmental factors. Data were corrected to standard atmospheric conditions (SAE J1349) to normalize the effects of ambient temperature and pressure. Key parameters recorded included wheel speed (km/h), wheel torque (N·m), and calculated wheel power (kW). The primary outputs reported are the maximum observed torque, maximum power, and the highest attainable wheel speed.

*2.4.2. Road Test*The road test is conducted to evaluate the performance of the E2W by obtaining data on maximum speed on the road and data on the driving cycle, including distance travelled and energy consumption per kilometer on a predefined urban route in Surabaya, East Java [50]. A smartphone-based GPS application recorded critical driving-cycle data, including speed profiles, distance travelled, and route characteristics [51]. Simultaneously, a digital joule meter with ±1% accuracy measured the battery's energy consumption.

Testing was performed in November 2024 under clear weather and dry road conditions. A licensed rider conducted all trials, following standard traffic regulations to replicate typical usage patterns. The same rider and tester were used across all vehicle configurations to minimize variability. Each test commenced with a fully charged battery. The road test yielded practical indicators of energy efficiency (kWh/km), driving range (km), and maximum achievable speed (km/h) under actual traffic conditions.

2.4.3. Limitations and Assumptions

This study assumed stable battery health and consistent ambient conditions across tests. Although efforts were made to maintain uniformity, minor variations in road surface, traffic dynamics, and wind conditions are inherent to real-world testing and represent unavoidable uncertainties. These limitations were mitigated through repeated trials and consistent rider assignment.

The findings are most directly applicable to the tested vehicle class and urban driving conditions, providing empirical insights relevant for similar conversion projects in developing urban contexts.

3. Results and Discussion

This section presents the experimental evaluation of the E2W converted from an ICE-TW. The assessment combines chassis dynamometer and road tests to provide a holistic understanding of performance, efficiency, and real-world road test applicability. Results are analyzed comparatively across powertrain configurations (hub motor, CVT, and single-gear ratio), benchmarked against typical specifications of entry-level commercial E2Ws, and critically discussed with reference to existing literature.

(a) (b) (c)

Figure 5. Electric two-wheeler conversion results: (a) hub / in-wheel (b) CVT (c) gear ratio

3.1. Electric Two-Wheeler Conversion Results

The retrofitted E2W retained consistent components across all units—including a 72 V, 20 Ah lithium-ion battery pack, a 3 kW BLDC motor, a MCU, and a DC-DC converter—ensuring that only the powertrain configuration varied. Figure 5 illustrates the integration of key components for hub motor, CVT, and gear-ratio-based systems. The uniform baseline enabled a fair performance comparison among the three systems.

3.2. Chassis Dynamometer Test Results

The dynamometer tests revealed distinct differences in wheel power, torque, and acceleration among the configurations. The testing setup for the chassis dynamometer is shown in Figure 6, which illustrates the standardized test configuration of the vehicle. The evaluation followed a steady-state power sweep protocol and data were collected to standard atmospheric conditions (SAE J1349).

The results from the chassis dynamometer test show that each powertrain configuration produces different performances in terms of power, wheel torque, and maximum speed. The results for the maximum speed test are shown in Figure 6 (a), while the power and wheel torque versus wheel speed data can be seen in Figure 6 (b). The CVT powertrain produced a maximum power of 3.906 kW, a maximum wheel torque of 180.908 N·m, and a maximum speed of 103 km/h. Meanwhile, the hub/in-wheel powertrain generated a maximum power of 4.246 kW, a maximum wheel torque of 151.04 N·m, and a maximum speed of 128 km/h. The gear ratio powertrain achieved a maximum power of 5.146 kW, a maximum wheel torque of 188.736 N·m, and a maximum speed of 128 km/h, the same as the hub powertrain.

From these results, it can be concluded that the highest maximum speed was achieved by the hub/in-wheel powertrain, which reached 128 km/h, surpassing the CVT that only reached 103 km/h. However, the gear ratio configuration showed the best performance regarding wheel torque and power, producing a maximum wheel torque of 188.736 N·m and a maximum power of 5.146 kW.

Further analysis of acceleration to maximum speed shows that the gear ratio powertrain recorded the fastest time to reach its peak speed, at 22 seconds, much faster than the other two powertrains. The hub/in-wheel and CVT powertrains each required more than 40 seconds to reach their maximum speeds. This indicates that the gear ratio configuration has an advantage in acceleration, although the hub/in-wheel system excels in maximum speed.

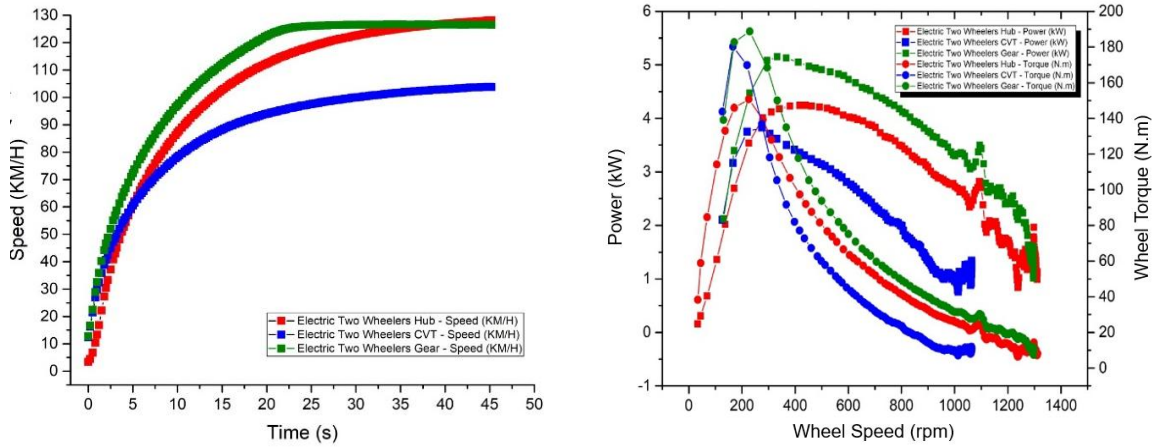

(a) (b)

Figure 6. Chassis dynamometer test results (a) speed performance (b) power and wheel torque performance

3.3. Road Test Results

On-road testing provided real-world insights into range and energy efficiency. Regarding maximum speed, the in-wheel (hub motor) configuration recorded the best performance, achieving 75 km/h, outperforming the CVT system (62 km/h) and the gear-ratio system (72 km/h). The advantage of the hub motor stems from its direct-drive mechanism, which minimizes energy loss during power transmission. Meanwhile, the gear-ratio system performed almost equally well at 72 km/h, indicating good power transmission efficiency despite using mechanical components. On the other hand, the CVT system recorded the lowest speed at 62 km/h, likely due to the inefficiencies of the CVT system when handling high loads.

In terms of range, the gear-ratio system showed the best performance with a range of 51.78 km, followed by the hub motor (43.71 km) and the CVT system (35.57 km). The gear-ratio system's superior range can be attributed to its ability to distribute torque optimally and minimize energy waste. The hub motor's middle position indicates a trade-off between speed and efficiency, while the CVT system's poorest performance underscores the high energy consumption in this system.

Energy consumption analysis revealed that the gear-ratio system was the most efficient, consuming 37.03 km/kWh, followed by the hub motor (31.25 km/kWh) and CVT (25 km/ kWh). These findings align with the performance trends observed in the other parameters, with the gear-ratio system exhibiting the best energy efficiency while the CVT system recorded the highest energy consumption.

3.4. Comparative Analysis, Trade-offs, and Benchmarking

The comparative performance of the three powertrain configurations under both dynamometer and road test conditions is summarized in Table 2. On the dynamometer, the gear ratio system exhibited the highest peak power (5.146 kW) and wheel torque (188.74 N·m), along with the fastest acceleration to maximum speed (22 s). In contrast, the hub motor achieved the highest maximum wheel speed (128 km/h), surpassing both the gear ratio and CVT configurations. Road testing reinforced these contrasts: the hub motor recorded the best on-road top speed (75 km/h), whereas the gear ratio system achieved the longest mileage (51.78 km) and the highest energy efficiency (37.03 km/kWh). The CVT configuration consistently underperformed in both dynamometer and road tests, indicating inherent limitations in adapting CVT mechanics to EV torque profiles.

The radar chart in Figure 7 highlights the multi-dimensional trade-offs among configurations. The hub motor excels in top-speed and acceleration metrics, making it suitable for urban commuting with frequent stop-and-go requirements. However, its simplicity comes at the cost of reduced energy efficiency. The gear ratio system demonstrates superior range and energy efficiency, emphasizing its suitability for long-distance or commercial delivery use cases, albeit with increased mechanical complexity. The CVT, while historically advantageous for ICE vehicles, exhibits limited compatibility with EV torque characteristics and requires substantial innovation (e.g., friction reduction, adaptive control strategies) to be competitive in electrified applications.

Voltage and motor power further influence these trade-offs. Higher voltage systems (e.g., 72V) increase peak power and acceleration but may slightly reduce energy efficiency in urban driving cycles. Similarly, higher-rated motors (3000W) improve performance on steep gradients but consume more energy per km, demonstrating the inherent trade-off between performance and range.

Table 2. The comparative analysis

Test	Performance	Powertrain Configuration		
		CVT	**In-wheel**	**Gear Ratio**
Dynamometer Test	Peak Power (kW)	3.906	4.246	5.146
	Peak Wheel Torque (N.m)	180.91	151.04	188.74
	Maximum Wheel Speed (km/h)	103	128	128
	Acceleration to Maximum Speed (s)	>40	>40	22
Road Test	Maximum Speed (km/h)	62	75	72
	Mileage (km)	35.57	43.71	51.78
	Energy Consumption (km/kWh)	25	31.25	37.03

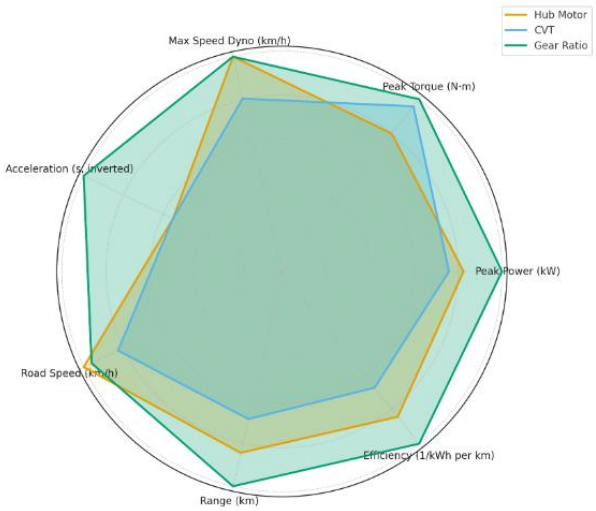

Figure 7. Radar chart comparison of hub, CVT, and gear ratio configurations across key performance dimensions

Benchmarking against the study by [14], which reported energy consumption of 17.8–18.5 km/kWh for a 3.5 kW electric scooter with a 1:6 gear ratio and 3 kWh battery, demonstrates substantial improvements in the present study: CVT achieved 25 km/kWh (+37.7%), hub motor 31.3 km/kWh (+72.2%), and gear ratio 37.0 km/kWh (+104%). When normalized to a 3 kWh battery, projected ranges were 75 km (CVT), 93.8 km (hub), and 111.1 km (gear ratio), exceeding the 53–55 km range reported in [14]. Conversely, applying [14]'s consumption rates to the 1.44 kWh battery used in this study would predict only 25–26 km, well below the experimentally measured 51.8 km for the gear ratio configuration.

Experimental measurements were subject to ±3% uncertainty due to dynamometer calibration, sensor accuracy, and environmental variability during road testing (temperature, wind, surface conditions). Internal consistency between predicted and measured range (−2.9% deviation for the gear ratio configuration) confirms the robustness of the experimental methodology.

The observed performance improvements can be attributed to optimized gear ratios, lower rolling resistance, reduced curb mass, and variations in test conditions. These trends confirm that gear ratio tuning and lightweight design are critical for maximizing range and efficiency. The multi-dimensional trade-off framework also corroborates previous findings that hub motors favor high-speed agility, whereas geared systems optimize energy efficiency and torque delivery.

Overall, the comparative and benchmarking analysis demonstrates that all three configurations are technically viable for E2W applications, but suitability depends on specific use-case priorities. Hub motors are preferable for urban commuting with frequent acceleration demands, gear ratio systems for efficiency- and range-oriented applications, and CVT configurations require further innovation to be competitive. These insights provide a foundation for optimizing powertrain selection and vehicle design to enhance practical performance and energy efficiency in emerging EV markets.

4. Conclusion

This study systematically evaluated three electric powertrain configurations—hub motor, single-gear ratio, and CVT—for ICE motorcycle conversions through dynamometer and real-road testing. The results identified the single-gear ratio system as the most efficient and best-performing configuration, achieving a wheel power of 5.146 kW, a peak wheel torque of 188.74 N·m, 0–128 km/h acceleration in 22 seconds, and the longest range of 51.78 km with an energy consumption of only 0.027 kWh/km. In contrast, the hub motor demonstrated moderate performance, while the CVT exhibited the lowest efficiency and shortest range. Therefore, this research provides critical evidence that the single-gear ratio powertrain is the optimal solution for accelerating the sustainable electrification of motorcycles, directly supporting national energy independence and emission reduction goals. Future work should

focus on higher-voltage systems, advanced control strategies, condition-specific testing, and the development of modular conversion kits to further enhance performance and enable large-scale adoption within Indonesia's motorcycle electrification efforts.

Acknowledgment
The author gratefully acknowledges the support from the *Center for Research and Innovation on Advanced Transportation Electrification (CReATE) – Politeknik Elektronika Negeri Surabaya*, whose resources, guidance, and collaborative environment have significantly contributed to the successful completion of this research.

References

[1] Kene R, Olwal T, van Wyk BJ. Sustainable electric vehicle transportation. Sustainability (Switzerland) 2021;13:1–16. https://doi.org/10.3390/su132212379.

[2] Choi S, Kwak K, Yang S, Lim S, Woo JR. Effects of policy instruments on electric scooter adoption in Jakarta, Indonesia: A discrete choice experiment approach. Economic Analysis and Policy 2022;76:373–84. https://doi.org/10.1016/j.eap.2022.08.015.

[3] Martias, Purwanto W, Handanu OJ, Baharudin A, Andrizal. Analysis of Modified Exhaust Tip Geometry on Flow Behavior and Backpressure in Car Exhaust Systems for Electricity Harvesting. Advance Sustainable Science, Engineering and Technology 2025;7:1–15. https://doi.org/10.26877/2dw2wx35.

[4] Hidayat HR, Irawan MZ, Rizki M, Aurarisa I. Exploring the determinants of electric motorcycle adoption and changes in travel behavior: Insights from Indonesia. Travel Behaviour and Society 2026;42. https://doi.org/10.1016/j.tbs.2025.101121.

[5] Guerra E. Electric vehicles, air pollution, and the motorcycle city: A stated preference survey of consumers' willingness to adopt electric motorcycles in Solo, Indonesia. Transportation Research Part D: Transport and Environment 2019;68:52–64. https://doi.org/10.1016/j.trd.2017.07.027.

[6] Schneider F, Castillo Castro DS, Weng KC, Shei CH, Lin HT. Comparative Life Cycle Assessment (LCA) on battery electric and combustion engine motorcycles in Taiwan. Journal of Cleaner Production 2023;406:1–9. https://doi.org/10.1016/j.jclepro.2023.137060.

[7] al Irsyad MI, Firmansyah AI, Harisetyawan VTF, Supriatna NK, Gunawan Y, Jupesta J, et al. Comparative total cost assessments of electric and conventional vehicles in ASEAN: Commercial vehicles and motorcycle conversion. Energy for Sustainable Development 2025;85:101599. https://doi.org/10.1016/j.esd.2024.101599.

[8] Presiden Republik Indonesia. Peraturan Presiden Republik Indonesia Nomor 79 Tahun 2023 tentang Perubahan atas Peraturan Presiden Nomor 55 Tahun 2019 tentang Percepatan Program Kendaraan Bermotor Listrik Berbasis Baterai (Battery Electric Vehicle) untuk Transportasi Listrik. 2023.

[9] Kementerian ESDM. Peraturan Menteri ESDM Nomor 1 Tahun 2023 Tentang Penyediaan Infrastruktur Pengisian Listrik untuk Kendaraan Bermotor Listrik Berbasis Baterai. 2023.

[10] Kementerian Perindustrian. Peraturan Menteri Perindustrian Nomor 21 Tahun 2023 tentang Perubahan atas Peraturan Menteri Perindustrian Nomor 6 Tahun 2023 tentang Pedoman Pemberian Bantuan Pemerintah Untuk Pembelian Kendaraan Bermotor Listrik Berbasis Baterai Roda Dua. 2023.

[11] UN. SDGs Report 2023. The Sustainable Development Goals Report 2023: Special Edition 2023:80.

[12] Tripathi SK, Kant R, Shankar R. Investigating the electric vehicle adoption initiatives for achieving sustainable development goals. Sustainable Futures 2025;9:100469. https://doi.org/10.1016/j.sftr.2025.100469.

[13] Rafiq F, Parthiban ES, Rajkumari Y, Adil M, Nasir M, Dogra N. From Thinking Green to Riding Green: A Study on Influencing Factors in Electric Vehicle Adoption. Sustainability (Switzerland) 2024;16:1–16. https://doi.org/10.3390/su16010194.
[14] Yuniarto MN, Wiratno SE, Nugraha YU, Sidharta I, Nasruddin A. Modeling, Simulation, and Validation of An Electric Scooter Energy Consumption Model: A Case Study of Indonesian Electric Scooter. IEEE Access 2022;10:48510–22. https://doi.org/10.1109/ACCESS.2022.3171860.
[15] Eccarius T, Lu CC. Powered two-wheelers for sustainable mobility: A review of consumer adoption of electric motorcycles. International Journal of Sustainable Transportation 2020;14:215–31. https://doi.org/10.1080/15568318.2018.1540735.
[16] Badan Pusat Statistik (BPS). Jumlah Kendaraan Bermotor Menurut Provinsi dan Jenis Kendaraan (unit), 2023 2024. https://www.bps.go.id/id/statistics-table/3/VjJ3NGRGa3dkRk5MTlU1bVNFOTVVbmQyVURSTVFUMDkjMw==/jumlah-kendaraan-bermotormenurut-provinsi-dan-jenis-kendaraan--unit---2023.html (accessed May 26, 2025).
[17] Charoen-amornkitt P, Nantasaksiri K, Ruangjirakit K, Laoonual Y. Energy consumption and carbon emission assessment of battery swapping systems for electric motorcycle. Heliyon 2023;9:e22887. https://doi.org/10.1016/j.heliyon.2023.e22887.
[18] Asosiasi Industri Sepeda Motor Indonesia. Statistics Distribution of Motorcycle Selling in Indonesia 2022. https://www.aisi.or.id/statistic/ (accessed December 30, 2024).
[19] Ardiansyah K, Suwahyo. Pengaruh Lebar V-Belt pada Sistem CVT Terhadap Performa Mesin. Automotive Science and Education Journal 2020;9:25–30.
[20] Tavares AA, Fornasa I, Cutipa-Luque JC, Ernesto Ponce Saldias C, Bianchi Carbonera LF, Elias Bretas De Carvalho B. Power Losses Analysis and Efficiency Evaluation of an Electric Vehicle Conversion. 2018 IEEE International Conference on Electrical Systems for Aircraft, Railway, Ship Propulsion and Road Vehicles and International Transportation Electrification Conference, ESARS-ITEC 2018 2018:1–6. https://doi.org/10.1109/ESARS-ITEC.2018.8607322.
[21] Manica L, Croitorescu V. Smart ForTwo electric conversion. Joint International Conference - ACEMP 2015: Aegean Conference on Electrical Machines and Power Electronics, OPTIM 2015: Optimization of Electrical and Electronic Equipment and ELECTROMOTION 2015: International Symposium on Advanced Electromechanical Moti 2016:731–6. https://doi.org/10.1109/OPTIM.2015.7426996.
[22] Aggarwal A, Chawla VK. A sustainable process for conversion of petrol engine vehicle to battery electric vehicle: A case study. Materials Today: Proceedings 2020;38:432–7. https://doi.org/10.1016/j.matpr.2020.07.617.
[23] Mohammed AS, Olalekan Salau A, Sigweni B, Zungeru AM. Conversion and performance evaluation of petrol engine to electric powered three-wheeler vehicle with an onboard solar charging system. Energy Conversion and Management: X 2023;20. https://doi.org/10.1016/j.ecmx.2023.100427.
[24] Rusli MR, Nugroho MAB, Jati MP, Toar H, Jaya A. Design and simulation of BLDCM drives using resolver. AIP Conference Proceedings 2023;2654:1–9. https://doi.org/10.1063/5.0114238.
[25] López I, Ibarra E, Matallana A, Andreu J, Kortabarria I. Next generation electric drives for HEV/EV propulsion systems: Technology, trends and challenges. Renewable and Sustainable Energy Reviews 2019;114:109336. https://doi.org/10.1016/j.rser.2019.109336.
[26] Chau KT, Chan CC, Liu C. Overview of permanent-magnet brushless drives for electric and hybrid electric vehicles. IEEE Transactions on Industrial Electronics 2008;55:2246–57. https://doi.org/10.1109/TIE.2008.918403.
[27] Chawrasia SK, Das A, Chanda CK, Banerjee S. Design, analysis and comparative study of Hub motor for an electric bike. IET Conference Proceedings 2020;2020:242–7. https://doi.org/10.1049/icp.2021.1179.

[28] Baskar S, Ruban M, Nethaji G. Impact of C 45 material manual gear transmissions in two wheeler. Materials Today: Proceedings 2022;69:665–7. https://doi.org/10.1016/j.matpr.2022.06.549.
[29] Yan H Sen, Wu YC. A novel design of a brushless DC motor integrated with an embedded planetary gear train. IEEE/ASME Transactions on Mechatronics 2006;11:551–7. https://doi.org/10.1109/TMECH.2006.882985.
[30] Shah NP, Hirzel AD, Cho B. Transmissionless selectively aligned surface-permanent-magnet BLDC motor in hybrid electric vehicles. IEEE Transactions on Industrial Electronics 2010;57:669–77. https://doi.org/10.1109/TIE.2009.2036022.
[31] Yang K, Damerla R, Awtar S. Design of a Novel Linkage-Based Active Continuously Variable Transmission for Anthropomorphic Prosthetic and Robotic Hands. IEEE/ASME International Conference on Advanced Intelligent Mechatronics, AIM 2022;2022-July:76–82. https://doi.org/10.1109/AIM52237.2022.9863415.
[32] Firmansyah AI, Supriatna NK, Gunawan Y, Setiadanu GT, Slamet. Performance Testing of Electric Motorcycle Conversion. 7th International Conference on Electric Vehicular Technology, ICEVT 2022 - Proceeding 2022:165–8. https://doi.org/10.1109/ICEVT55516.2022.9924921.
[33] Plus M. Vario Series Paling Laris, Lebih dari 5.000 Unit Motor Honda Terjual di JFK 2025 2025. https://www.motorplus-online.com/read/254273817/vario-series-paling-laris-lebih-dari-5000-unit-motor-honda-terjual-di-jfk-2025 (accessed July 1, 2025).
[34] ANTARA. 10 sepeda motor terlaris 2017 2018. https://otomotif.antaranews.com/berita/677177/10-sepeda-motor-terlaris-2017 (accessed May 3, 2025).
[35] Asosiasi Industri Sepeda Motor Indonesia. Penjualan Unit Motor Berkapasitas 125cc Pada Tahun 2017. 2017.
[36] Hibatullah NA, Setiawan R, Bandung T. Drive system selection and the development of chassis structure basic design for medium-sized urban electric bus. Jurnal Polimesin 2024;22:361–70.
[37] M. S. H. Lipu et al. Battery Management, Key Technologies, Methods, Issues, and Future Trends of Electric Vehicles: A Pathway toward Achieving Sustainable Development Goals. Batteries 2022;8:119. https://doi.org/https://doi.org/10.3390/batteries8090119.
[38] Pistoia G. Chapter 5 - Vehicle Applications: Traction and Control Systems. Battery Operated Devices and Systems, Elsevier; 2009, p. 321–78. https://doi.org/10.1016/b978-0-444-53214-5.00005-4.
[39] Taizhou Quanshun Motor Co Ltd. SiAECOSYS/VOTOL Programmable EM150sp 72V 150A 100KPH Controller for 1-5kW Electric Scooter Bike 2022. http://www.cnqsmotor.com/en/article_read_1228.html (accessed January 3, 2025).
[40] Kukovinets O V., Sidorov KM, Yutt VE. Isolated step-down DC -DC converter for electric vehicles. IOP Conference Series: Materials Science and Engineering 2018;315:1–7. https://doi.org/10.1088/1757-899X/315/1/012015.
[41] Pang Z, Ren X, Xiang J, Chen Q, Ruan X, Chen W. High-frequency DC-DC converter in electric vehicle based on GaN transistors. ECCE 2016 - IEEE Energy Conversion Congress and Exposition, Proceedings, 2016, p. 1–7. https://doi.org/10.1109/ECCE.2016.7855159.
[42] Ranjith S, Vidya V, Kaarthik RS. An Integrated EV Battery Charger with Retrofit Capability. IEEE Transactions on Transportation Electrification 2020;6:985–94. https://doi.org/10.1109/TTE.2020.2980147.
[43] Mohanraj D, Aruldavid R, Verma R, Sathiyasekar K, Barnawi AB, Chokkalingam B, et al. A Review of BLDC Motor: State of Art, Advanced Control Techniques, and Applications. IEEE Access 2022;10:54833–69. https://doi.org/10.1109/ACCESS.2022.3175011.
[44] Behera RK, Kumar R, Bellala SM, Raviteja P. Analysis of electric vehicle stability effectiveness on wheel force with BLDC motor drive. Proceedings - 2018 IEEE International Conference on

Industrial Electronics for Sustainable Energy Systems, IESES 2018 2018;2018-Janua:195–200. https://doi.org/10.1109/IESES.2018.8349873.
[45] Lee TY, Seo MK, Kim YJ, Jung SY. Motor Design and Characteristics Comparison of Outer-Rotor-Type BLDC Motor and BLAC Motor Based on Numerical Analysis. IEEE Transactions on Applied Superconductivity 2016;26:1–6. https://doi.org/10.1109/TASC.2016.2548079.
[46] Ammari O, Majdoub K El, Giri F. Modeling and control of a half electric vehicle including an inverter, an in-wheel BLDC motor and Pacejka's tire model. IFAC-PapersOnLine 2022;55:604–9. https://doi.org/10.1016/j.ifacol.2022.07.378.
[47] Rinderknecht S, Meier T. Electric power train configurations and their transmission systems. SPEEDAM 2010, 2010, p. 1564–8. https://doi.org/10.1109/SPEEDAM.2010.5542276.
[48] Spanoudakis P, Tsourveloudis NC. On the efficiency of a prototype continuous variable transmission system. 2013 21st Mediterranean Conference on Control and Automation, MED 2013 - Conference Proceedings, 2013, p. 290–5. https://doi.org/10.1109/MED.2013.6608736.
[49] Plaza B. SUPER DYNO 50 LA 2022. https://brtplaza.com/c51ce410c124a10e0db5e4b97fc2af39-super-dyno-50-la-gudang-brt.html (accessed January 3, 2025).
[50] Yuniarto, M N, Sidharta I, Wiratno SE, Nugraha YU, Asfani DA. Indonesian Electric Motorcycle Development: Lessons from innovation-based concept implementation on the design and production of the first Indonesian electric motorcycle. IEEE Electrification Magazine 2022;22:2325–5897. https://www.doi.org/10.1109/MELE.2021.3139247.
[51] Rechkemmer SK, Zang X, Boronka A, Zhang W, Sawodny O. Utilization of Smartphone Data for Driving Cycle Synthesis Based on Electric Two-Wheelers in Shanghai. IEEE Transactions on Intelligent Transportation Systems 2021;22:876–86. https://doi.org/10.1109/TITS.2019.2961179.